

SUPPLEMENTAL MATERIAL

Eruption dynamics leading to a volcanic thunderstorm—The January 2020 eruption of Taal volcano, Philippines

Alexa R. Van Eaton¹, Cassandra M. Smith², Michael Pavlonis³, and Ryan Said⁴

¹U.S. Geological Survey, Cascades Volcano Observatory, Vancouver, Washington, USA

²Alaska Volcano Observatory, Anchorage, Alaska, USA

³NOAA/NESDIS Center for Satellite Applications and Research, Advanced Satellite Products Branch, Madison, Wisconsin, USA

⁴Vaisala, Inc., Boulder Operations, Louisville, Colorado USA

1. CALCULATING ERUPTION RATE FROM UMBRELLA EXPANSION

We used the volcanic umbrella cloud spreading model of Pouget et al. (2013) and Costa et al. (2013) to determine the time-averaged mass eruption rate during a time period of sustained, intense eruption during the Taal eruption from 7:43–10:03 UTC. Umbrella cloud areas were extracted from Himawari-8 satellite in the thermal infrared 11 μm band using six different contours of infrared brightness temperature, from -23 to -73°C in 10° increments. Areas within the isotherm lines were converted to equivalent circular radii and reported as average, maximum, and minimum values (Supplementary Fig. S1; Supplementary Dataset). Note there is a gap in the satellite data at 14:43 UTC. To provide a more accurate time stamp for each satellite image, we identified when the scan line reached Taal volcano, rather than using the image acquisition start time. The satellite view of Taal is only about 28° off of nadir, so parallax had minimal effect on apparent cloud geometry. Assuming a constant volumetric flow rate of gas and particles into the umbrella region, the umbrella cloud radius R (in km) expands through time according to:

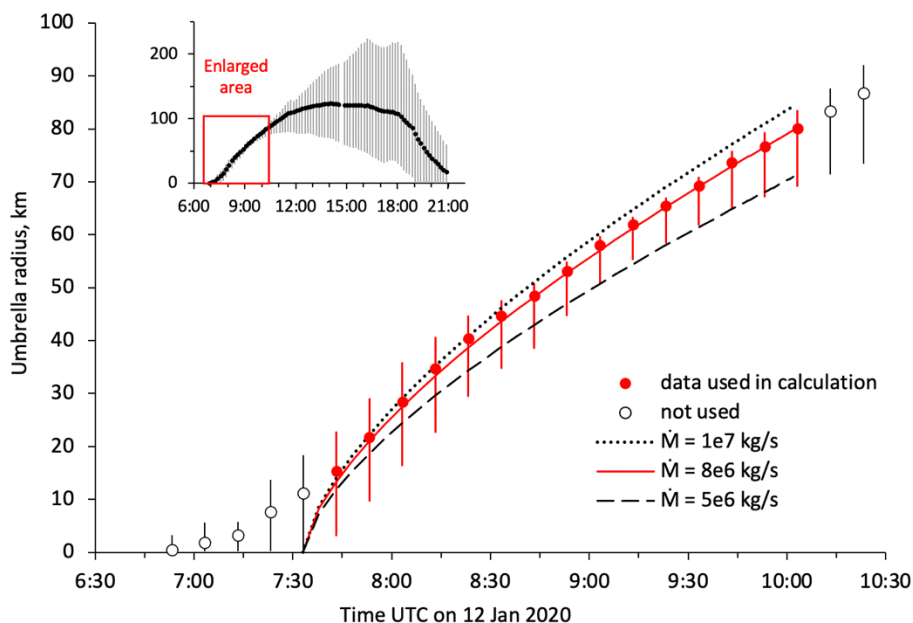
$$R = \left(\frac{3\lambda NV}{2\pi} \right)^{1/3} t^{2/3}, \quad (\text{Eq. S1})$$

where λ is an umbrella shape factor taken as 0.2 after Suzuki and Koyaguchi (2009), N is the Brunt-Vaisala frequency of the atmosphere in the umbrella region, calculated to be 0.009 s^{-1} from 10–17 km above sea level using the atmospheric sounding measurements from Mactan, Philippines, and t is time in s since the onset of sustained umbrella development, taken as 7:33 UTC. V is the volumetric flow rate into the umbrella region ($\text{m}^3 \text{ s}^{-1}$), as defined by Webster et al. (2020):

$$V = C \sqrt{k} \frac{\dot{M}^{3/4}}{N^{5/4}}, \quad (\text{Eq. S2})$$

where C is an empirical constant taken as $4.3 \times 10^2 \text{ m}^3 \text{ kg}^{-3/4} \text{ s}^{-3/2}$ for tropical eruptions (Costa et al., 2013; erratum), k is the dimensionless radial entrainment coefficient of air ingested into the rising plume, taken as 0.1 (Suzuki and Koyaguchi, 2009), and \dot{M} is the mass eruption rate in kg s^{-1} . We explored several different methods of determining mass eruption rate by using umbrella expansion (Fig. S1), empirical plume height scaling (Eq. 1 in main text), and 1-D modeling (Fig.

S2) to estimate an uncertainty of $\sim 75\%$ on our reported values and propagated that uncertainty to the calculations of erupted mass and volume.

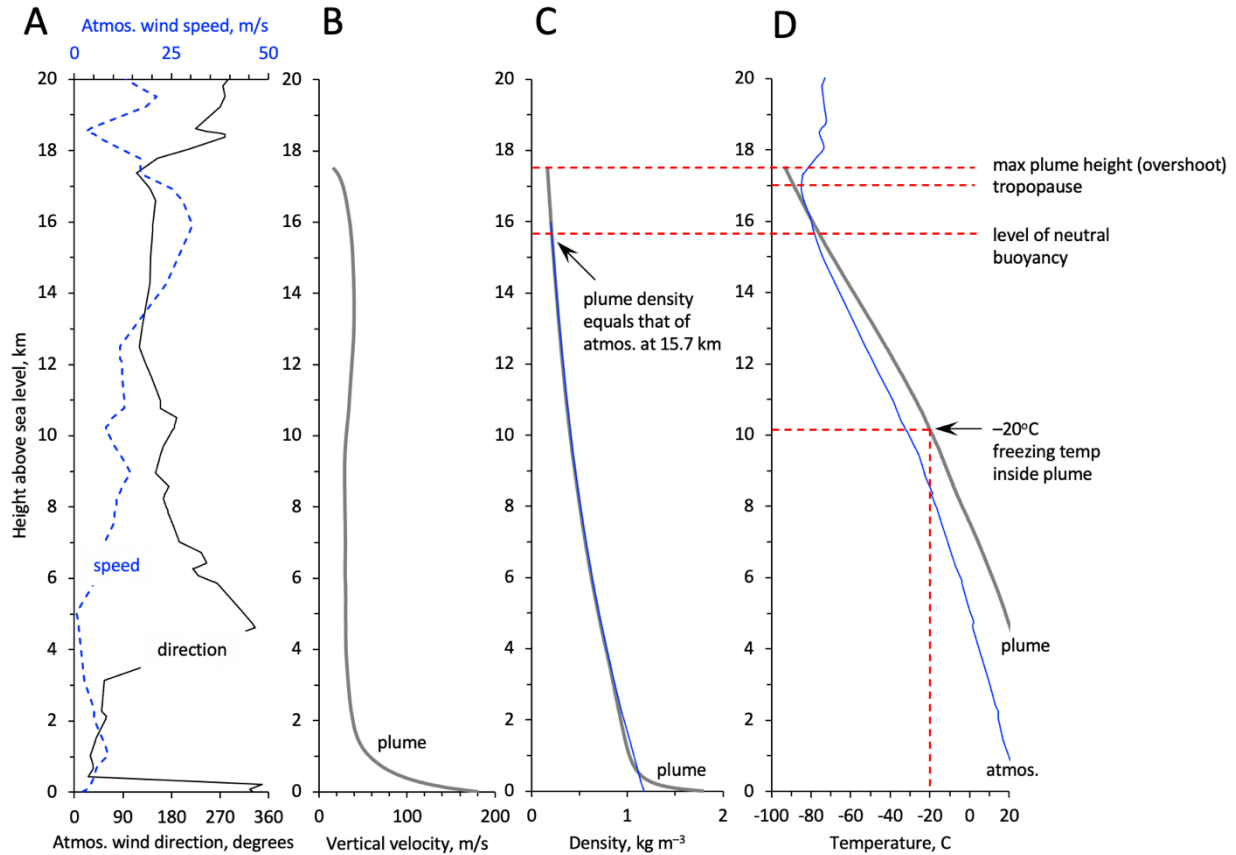


Supplementary Fig. S1. Timeline of Taal’s umbrella cloud radii derived from Himawari-8 satellite brightness temperatures. Inset shows the full time series from 6:00–21:00 UTC. Circles give the cloud radii averaged from six isotherms, with error bars giving maximum and minimum values. The top of each error bar shows radius of the largest/outer isotherm (-23°C) and bottom of each error bar shows radius of the smallest/inner isotherm (-73°C). Red circles indicate data points used in the calculation, based on satellite images showing intensification and sustained upwind growth of the umbrella cloud. These points were used to calculate the time-averaged mass eruption rate from 7:43–10:03 UTC. The curves show growth rates calculated from Eqs. S1 and S2 by assuming three different mass eruption rates (\dot{M}) and an onset time (intensification) of 7:33 UTC. The best fit \dot{M} to the average umbrella radii is $8 \times 10^6 \text{ kg}^{-\text{s}}$ (red curve).

2. THERMODYNAMIC MODELING OF THE VOLCANIC PLUME

The 1-D volcanic plume model *Plumeria* (Mastin, 2007; Mastin, 2014) was used to examine thermodynamic properties of Taal’s water-rich volcanic plume. *Plumeria* calculates mean properties of steady state volcanic plumes as a function of height, accounting for water phase changes such as condensation and freezing (Mastin, 2007), and bending of the plume due to the background wind field (Mastin, 2014). For atmospheric inputs, we used the sounding data at 12:00 UTC on 12 Jan 2020 from Mactan, Philippines, which is 500 km south of Taal (<http://weather.uwyo.edu/upperair/sounding.html>). These atmospheric measurements agree well with modeled atmospheric profiles directly over Taal volcano from NCEP/NCAR 2.5 deg, 6 hourly, global Reanalysis (<https://www.ready.noaa.gov/READYamet.php>).

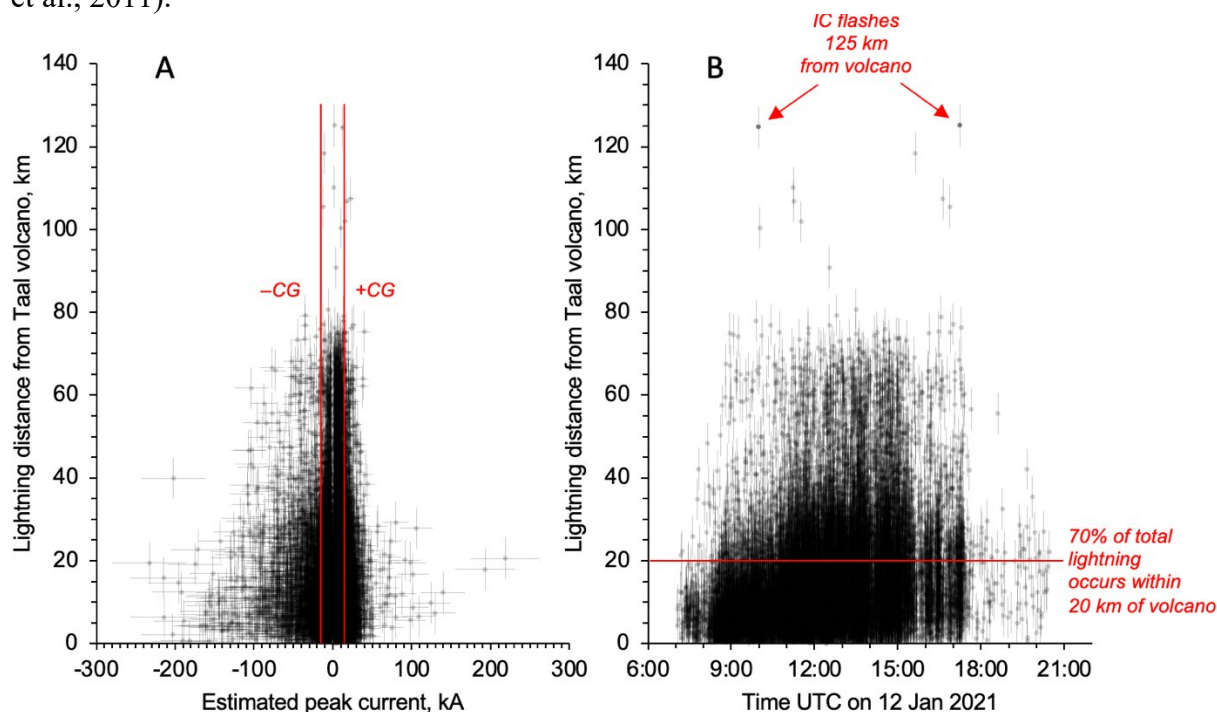
We modeled a plume with the maximum observed height of 17.5 km asl, an initial magma temperature of 1000°C, 3 wt.% magmatic water, 20 wt.% surface water incorporated from the lake, initial plume diameter of 150 m, and initial vertical velocity of 180 m s⁻¹. These parameters resulted in a mass eruption rate of 5.7 x10⁶ kg s⁻¹, which is within 60% of the time-averaged eruption rate determined from plume height scaling over the full eruptive sequence (Eq. 1 in main text).



Supplementary Fig. S2. Properties of the background atmosphere and results of thermodynamic modeling of the volcanic plume using the 1-D model Plumeria (bold grey curves in B–D). (A) shows atmospheric wind speed and direction from weather sounding at Mactan, Philippines, 12:00 UTC on 12 Jan 2020. A wind direction of 180 degrees indicates winds blowing from the south. (B) Modeled profile of vertical velocities shows convective updrafts >20–30 m/s in the upper plume. (C) Modeled bulk density of the volcanic plume equals that of the background atmosphere ~15.7 km asl. This level of neutral buoyancy roughly approximates the altitude where the umbrella cloud spreads out radially (Suzuki and Koyaguchi, 2009). (D) Modeled temperatures indicate the plume would have cooled from 1000°C to –20°C above 10 km asl, which is where ice formation is expected to occur in the presence of ash particles (Schill et al., 2015).

3. DETAILS OF LIGHTNING DATA AND PHOTOGRAPHS

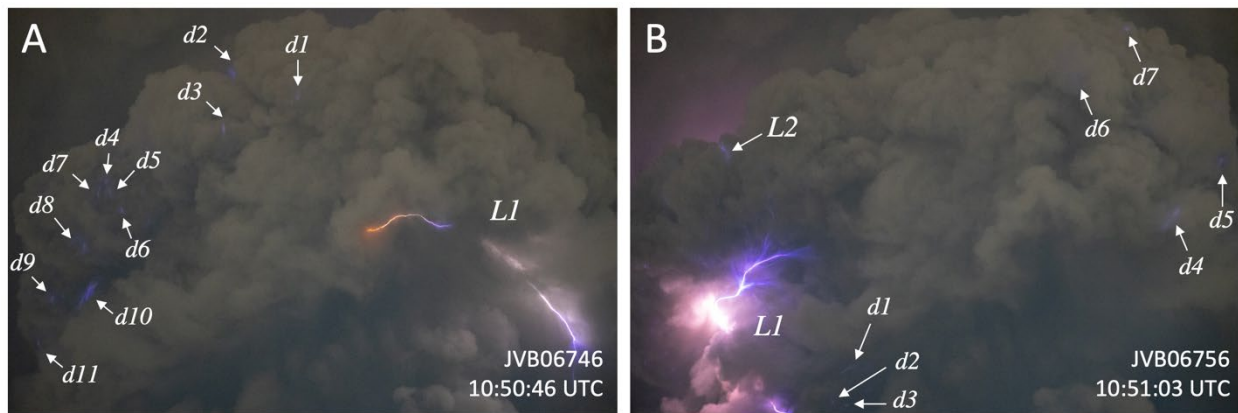
In addition to producing visible energy, lightning emits a broad spectrum of electromagnetic radiation, including radio waves in the very low frequency (VLF) band from 3–30 kHz. This VLF energy propagates thousands of kilometers away at the speed of light, conducted by the Earth-ionosphere waveguide (Said et al., 2010). Vaisala’s GLD360 uses ground-based radio antennas to determine 2-D lightning locations (not including altitude). It is the only global detection system using both time-of-arrival and magnetic-direction finding at three or more sensors, which results in an improved yield because fewer sensors are required to detect each event (Said and Murphy, 2016). Flashes have a median, radial location uncertainty of 2.5 km, and the majority of locations are constrained within 5 km (Said et al., 2013; their Fig. 3). The timing uncertainty is ~10 microseconds, and detection efficiency in the range of 67–80% for cloud-to-ground lightning (Said et al., 2010; Said and Murphy, 2016). For this study, individual lightning strokes were grouped into a single parent flash if they occurred within 1 second and 20 km of each other, with an additional constraint of a 500 ms inter-stroke interval tolerance. Estimates of lightning peak currents were modeled from the strength of the VLF magnetic field. The validation study of Said et al. (2013) compared 353 million flashes detected by the U.S. National Lightning Detection Network, showing that the GLD360 has a mean error of ~20% on the estimates of peak current, with greater uncertainties for weaker flashes. We used the method of Biagi et al. (2007) to classify flashes as cloud-to-ground (CG) if peak current magnitudes were ≥ 15 kA (Supplementary Fig. S3). Biagi et al. (2007) found that flashes exceeding 15 kA were more likely to be CG than IC and ~95% of flashes exceeding 20 kA were CG lightning. We acknowledge that this is a simplifying assumption of our study, but one that has been commonly used in lightning classification over the past decade (e.g., Cummins and Murphy, 2009; Schultz et al., 2011).



Supplementary Fig. S3. Lightning detected by the GLD360 network for the 2020 Taal eruption ($n=18,795$), showing (A) estimated peak currents with distance, and (B) time series of lightning

location distances from Taal volcano. Error bars show a ~20% uncertainty for peak currents and 5 km uncertainty on locations. Vertical red lines in (A) denote the Biagi et al. classification of cloud-to-ground versus in-cloud lightning. Horizontal line in (B) indicates the 20 km distance from Taal volcano, where 70% of total lightning occurred. Note that at least two flashes occurred 125 km from Taal, classified as in-cloud lightning.

Photographs were taken by Joshua Bobadilla from Batangas City, in a residential neighborhood located ~30 km SE of Taal volcano in the Philippines (see Fig. 1 in main text). He used a Sony a6400 mirrorless camera and tripod on continuous shooting time lapse mode. The overview photo series (Fig. 1 B,C in main text) used a 16 mm focal length, 0.2 sec exposure time at f/4, aperture value 0.969, and ISO 2500, capturing ~4 images per second. The closeup photo series (Fig. 1 D–G in main text) used a 50 mm focal length with 1 sec exposure time at f/1.8, aperture value 1.696, and ISO 6400, capturing an image every 1–2 seconds. Our manual counts of lightning flashes identified the discrete lightning leaders in each frame, characterized by their high-intensity brightness, orange to white color, and/or sharply defined channel morphology. In contrast, faint blue filaments, flame-like shapes, or diffuse points of blue light were identified as streamer discharges using the morphology and color criteria of Lyons et al. (2003) and Soler et al. (2020). Note these tiny discharges (tens to hundreds of m) were counted separately from flashes if they were visually isolated from a lightning leader (Supplementary Fig. S4), which was relatively straightforward in the timelapse images because the leaders tend to appear much brighter than other discharges and illuminate the surrounding area even when they occur inside the cloud.



Supplementary Fig. S4. Examples showing how electrical discharges were counted in the closeup photo series. Lightning flashes were determined by the presence of a lightning leader, labeled ‘L’ in the images. Non-leader discharges are labeled ‘d,’ defined by their relatively faint, diffuse appearance and blue color. Image in (A) contains 1 lightning flash and 11 non-leader discharges; (B) contains 2 flashes and 7 non-leader discharges. Over the 60-sec time period from 10:50:15–10:51:15 there were 37 flashes and 319 non-leader discharges.

4. RELATIONSHIP BETWEEN PLUME HEIGHT AND LIGHTNING RATE

Studies of ordinary meteorological thunderstorms (Williams, 1985; Price and Rind, 1992) have parameterized the power-law relationship between maximum cloud height and lightning flash rate for continental and marine clouds:

$$F = \begin{cases} 3.44 \times 10^{-5} H^{4.9}, & \text{continental clouds} \\ 6.2 \times 10^{-4} H^{1.73}, & \text{marine clouds} \end{cases}, \text{ (Eq. S3)}$$

where F is lightning flashes per minute and H is cloud height in km above sea level, as reported in Price and Rind (1992; their Fig. 6). Solving for H gives:

$$H = \begin{cases} 8.15 F^{0.20}, & \text{continental clouds} \\ 71.47 F^{0.58}, & \text{marine clouds} \end{cases}, \text{ (Eq. S4)}$$

which is plotted in Fig. 2B in the main text (note: only the continental cloud curve shows up on the scale of the plot). This power law relationship was extended from meteorology to volcanic plumes by Prata et al. (2020) for the 2019 eruption of Anak Krakatau, Indonesia. Their analysis of satellite-derived plume heights and lightning detected by the ENGLN global lightning network revealed the following relationship:

$$H = 12.54 f^{0.05}, \text{ (Eq. S5)}$$

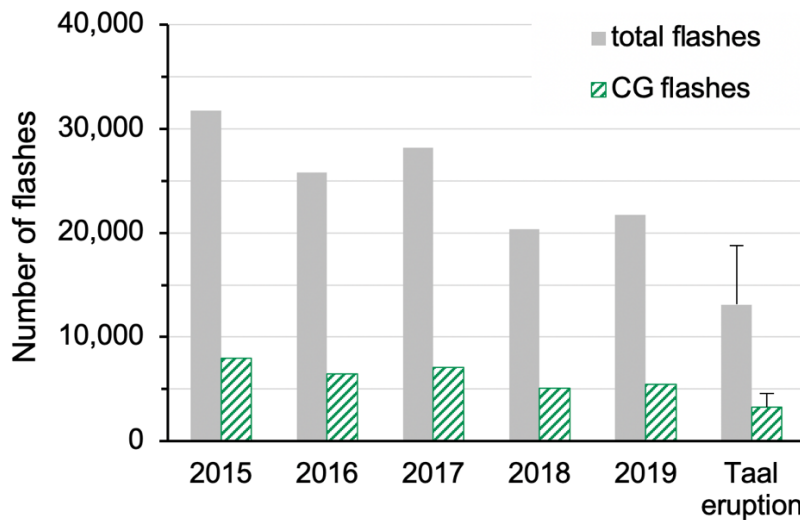
where f is flash rate in flashes per 10 minutes. Reformulating in terms of flash rate per minute to provide a form comparable to that of Price and Rind (1992) gives:

$$H = 14.07 F^{0.05}, \text{ (Eq. S6)}$$

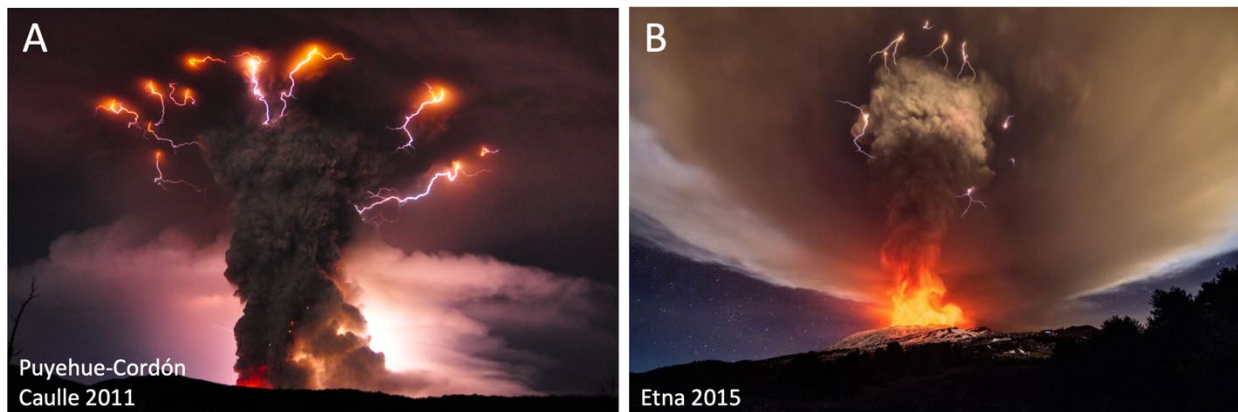
which is within uncertainty of the Taal plot shown in Fig. 2B of the main text. Our examination of Taal's maximum plume heights detected by Himawari-8 brightness temperatures and total lightning flash rates detected by the GLD360 network, reported in flashes min^{-1} (averaged between satellite passes every 10 min or 20 min) gives the following power-law relationship with an R^2 of 0.76:

$$H = 12.69 F^{0.08}, \text{ (Eq. S7)}$$

which minimizes the sum of squares in linear space and is based on 80 non-zero measurements (green curve in Fig. 2B of main text).



Supplementary Fig. S5. Comparison of Taal’s volcanic lightning to ordinary meteorological lightning in the region. Plot shows the number of lightning flashes detected by the GLD360 network within a 20 km radius of Taal volcano for each 1-year period from 2015–2019, compared to only 14 hours of lightning production during the climactic eruption of Taal in 2020. CG indicates cloud-to-ground lightning (green columns). Error bars on the Taal plots show all volcanic lightning associated with the eruption (within 200 km of the vent). Note that the eruption produced a significant fraction of the typical annual lightning budget for this region of the Philippines.



Supplementary Fig. S6. Long-exposure photos of other eruptions showing lightning activity concentrated at the base of the umbrella cloud. In context with our analysis of Taal’s lightning, the photos suggest that enhanced electrical activity at the umbrella cloud base may be a common phenomenon in large volcanic plumes. (A) Puyehue-Cordón Caulle, Chile, on 5 June 2011 by Daniel A. Basualto Alarcón (source: cover photo from the Oct 2018 issue of *Geology* <https://pubs.geoscienceworld.org/geology/issue/46/10>). (B) Etna, Italy, on 3 December 2015 by Marco Restivo (source: <https://www.forbes.com/sites/trevornace/2015/12/05/fire-lightning-mt-etna-erupts-sicily-ejecting-lava-air/?sh=3a26735d318d>).

SUPPLEMENTAL REFERENCES

- Biagi, C. J., Cummins, K. L., Kehoe, K. E., and Krider, E. P., 2007, National Lightning Detection Network (NLDN) performance in southern Arizona, Texas, and Oklahoma in 2003–2004: *Journal of Geophysical Research*, v. 112, D05208, doi:10.1029/2006jd007341.
- Costa, A., Folch, A., and Macedonio, G., 2013, Density-driven transport in the umbrella region of volcanic clouds: Implications for tephra dispersion models [Erratum published 17 Jun 2019]: *Geophysical Research Letters*, v. 40, doi:10.1002/grl.50942.
- Cummins, K. L., and Murphy, M. J., 2009, An Overview of Lightning Locating Systems: History, Techniques, and Data Uses, With an In-Depth Look at the U.S. NLDN: *IEEE Transactions on Electromagnetic Compatibility*, v. 51, p. 499-518, doi:10.1109/TEMC.2009.2023450.
- Lyons, W. A., Nelson, T. E., Armstrong, R. A., Pasko, V. P., and Stanley, M. A., 2003, Upward electrical discharges from thunderstorm tops: *Bulletin of the American Meteorological Society*, v. 84, p. 445-454, doi:10.1175/bams-84-4-445.
- Mastin, L. G., 2007, A user-friendly one-dimensional model for wet volcanic plumes: *Geochemistry, Geophysics, Geosystems*, v. 8, Q03014, doi:10.1029/2006GC001455.
- Mastin, L. G., 2014, Testing the accuracy of a 1-D volcanic plume model in estimating mass eruption rate: *Journal of Geophysical Research*, v. 119, p. 2474–2495, doi:10.1002/2013JD020604.
- Pouget, S., Bursik, M., Webley, P., Dehn, J., and Pavolonis, M., 2013, Estimation of eruption source parameters from umbrella cloud or downwind plume growth rate: *Journal of Volcanology and Geothermal Research*, v. 258, p. 100-112, doi:10.1016/j.jvolgeores.2013.04.002.
- Prata, A. T., Folch, A., Prata, A. J., Biondi, R., Brenot, H., Cimarelli, C., Corradini, S., Lapierre, J., and Costa, A., 2020, Anak Krakatau triggers volcanic freezer in the upper troposphere: *Scientific Reports*, v. 10, 3584, doi:10.1038/s41598-020-60465-w.
- Price, C., and Rind, D., 1992, A simple lightning parameterization for calculating global lightning distributions: *Journal of Geophysical Research*, v. 97, p. 9919–9933, doi:10.1029/92JD00719.
- Said, R., and Murphy, M., 2016, GLD360 upgrade: Performance analysis and applications: in *Proceedings, 24th International Lightning Detection Conference & 6th International Lightning Meteorology Conference*, San Diego, California, April 2016, 8 pp.

- Said, R. K., Inan, U. S., and Cummins, K. L., 2010, Long-range lightning geolocation using a VLF radio atmospheric waveform bank: *Journal of Geophysical Research*, v. 115, D23108, doi:10.1029/2010jd013863.
- Said, R. K., Cohen, M. B., and Inan, U. S., 2013, Highly intense lightning over the oceans: Estimated peak currents from global GLD360 observations: *Journal of Geophysical Research: Atmospheres*, v. 118, p. 6905-6915, doi:10.1002/jgrd.50508.
- Schill, G. P., Genareau, K., and Tolbert, M. A., 2015, Deposition and immersion-mode nucleation of ice by three distinct samples of volcanic ash: *Atmospheric Chemistry and Physics*, v. 15, p. 7523–7536, doi:10.5194/acp-15-7523-2015.
- Schultz, C. J., Petersen, W. A., and Carey, L. D., 2011, Lightning and severe weather: A comparison between total and cloud-to-ground lightning trends: *Weather and Forecasting*, v. 26, p. 744-755, doi:10.1175/waf-d-10-05026.1.
- Soler, S., Pérez-Invernón, F. J., Gordillo-Vázquez, F. J., Luque, A., Li, D., Malagón-Romero, A., Neubert, T., Chanrion, O., Reglero, V., Navarro-Gonzalez, J., Lu, G., Zhang, H., Huang, A., and Østgaard, N., 2020, Blue optical observations of narrow bipolar events by ASIM suggest corona streamer activity in thunderstorms: *Journal of Geophysical Research: Atmospheres*, v. 125, e2020JD032708, doi:10.1029/2020jd032708.
- Suzuki, Y. J., and Koyaguchi, T., 2009, A three-dimensional numerical simulation of spreading umbrella clouds: *Journal of Geophysical Research*, v. 114, B03209, doi:10.1029/2007jb005369.
- Webster, H. N., Devenish, B. J., Mastin, L. G., Thomson, D. J., and Van Eaton, A. R., 2020, Operational modelling of umbrella cloud growth in a Lagrangian volcanic ash transport and dispersion model: *Atmosphere*, v. 11, doi:10.3390/atmos11020200.
- Williams, E. R., 1985, Large-scale charge separation in thunderclouds: *Journal of Geophysical Research*, v. 90, p. 6013-6025, doi:10.1029/JD090iD04p06013.